Thin Solid Films xxx (2016) xxx–xxx

Contents lists available at ScienceDirect

Thin Solid Films

journal homepage: www.elsevier.com/locate/tsf

Comparison between single monomer versus gas mixture for the deposition of primary amine-rich plasma polymers

Cédric Vandenabeele [a,*], Madhuwanthi Buddhadasa [b], Pierre-Luc Girard-Lauriault [b], Rony Snyders [a,c]

[a] Laboratoire de Chimie des Interactions Plasma-Surfaces (ChIPS), CIRMAP, Université de Mons, 23 Place du Parc, 7000 Mons, Belgium
[b] Plasma Processing Laboratory, Department of Chemical Engineering, McGill University, 3610 University (Wong Building) Montreal, QC H3A 2B2, Montreal, Canada
[c] MateriaNova Research Center, Parc Initialis, 1 Avenue Nicolas Copernic, 7000 Mons, Belgium

ARTICLE INFO

Article history:
Received 19 May 2016
Received in revised form 26 July 2016
Accepted 4 August 2016
Available online xxxx

Keywords:
Plasma polymerization
Primary amine-rich polymer
Thin film
Chemical derivatization
Optical emission spectroscopy
X-ray photoelectron spectroscopy

ABSTRACT

Primary amine-based plasma polymer films (NH_2-PPFs) attract great attention due to their potential for various biomedical applications. In this context, in order to better understand the growth mechanism of such coatings, we investigate the impact of the precursor mixture on plasma chemistry and ultimately, on PPFs properties. PPFs are synthesized from both cyclopropylamine (CPA) and ammonia/ethylene (AmEt) mixture in low pressure (2.7 Pa) inductively-coupled plasma discharges, keeping the N/C ratio constant in the precursor flow rate. Optical emission spectroscopy (OES) is performed to study the plasma phase while PPFs chemistry is investigated by Fourier transform infrared spectroscopy and X-ray photoelectron spectroscopy (combined with chemical derivatization). The results show that, for similar energetic conditions, the use of CPA allows a better nitrogen incorporation in the film compared with the use of the AmEt mixture. This is attributed to the initial presence of C—N bonds in the CPA molecule. In addition, it is shown that primary amine retention decreases when the power increases due to a strong dehydrogenation of the monomers that promotes the formation of multiple and conjugated CN bonds. Using OES, etching reactions of the growing PPFs surfaces are highlighted and are shown to strongly influence the plasma chemistry.

1. Introduction

The synthesis of primary amine-rich surfaces has attracted great attention due to its potential for various applications in biotechnology, such as cell colonization [1], microfiltration membranes [2] or biosensor development [3–5]. These surfaces are well-known reactive platforms for the covalent immobilization of biomolecules [6]. Indeed, primary amine groups, being positively charged in aqueous environments at physiological pH values, are supposed to attract the negatively-charged molecules (e.g., fibronectin or vitronectin), as well as RGD peptides, which are important for cell adhesion and growth [7].

Different plasma processes have been reported to allow obtaining primary amine-rich surfaces. The simplest technique consists of grafting NH_2 groups by exposing the surface, for example, to an ammonia (NH_3) or a nitrogen/hydrogen (N_2/H_2) discharge [8]. However, this technique suffers from unstable functionalization due to reptation phenomena [6]. On the contrary, plasma polymerization is known to enhance the stability and reduce the ageing effect encountered in the grafting approach [9]. Different kinds of precursor have been used to synthesize the plasma polymer films (PPFs). Both single monomers (allylamine (AA) [10–12], diaminocyclohexane (DACH) [12–14], ethylenediamine (EDA) [12,15], heptylamine (HA) [12,16], cyclopropylamine (CPA) [9,17], …) and gas mixtures (N_2/ethylene (C_2H_4), NH_3/C_2H_4 [7,18], NH_3/acetylene (C_2H_2) [19], NH_3/butadiene (C_4H_6) [18], …) have been employed.

Based on this important set of data, it is preferable for some researchers to work with a single monomer that already contains the chemical group of interest to promote a better incorporation of this group in the deposited layer [7]. Nevertheless, for other groups, the use of a gas mixture allows a more flexible surface chemistry by tuning the monomer gas flow ratio [18]. It is well known that the chemical structure of the precursors has a direct impact on the physicochemical characteristics of the resulting PPF in "mild" plasma conditions of low or pulsed power [20,21]. However, the initial precursor structure is no more conserved when extensive molecular fragmentation occurs in the discharge (high power conditions), and one could think in this case that the nitrogen to carbon ratio in the precursor would prevail on the precursor structure.

Denis et al. [17] show for example that the retention of primary amine groups in PPFs deposited from two different isomeric precursors, namely AA vs CPA, only differs in low power conditions for which the monomer fragmentation leads to species of different nature. However, Ryssy et al. [12] show more recently, by studying both plasma and

* Corresponding author.
E-mail address: Cedric.Vandenabeele@umons.ac.be (C. Vandenabeele).

http://dx.doi.org/10.1016/j.tsf.2016.08.008
0040-6090/

thin film chemistries for four precursors having more different structure with well-distinct nitrogen to carbon ratios (AA, EDA, DACH and HA), that the choice of the precursor strongly influences the primary amine content and PPF stability whatever the energetic conditions, even if they conclude that the nitrogen to carbon ratio is not a good predictor of surface functionality. They correlate the primary amine retention to the binding energies implied in the different molecules and to the stability of the resultant precursor ions and other ionic oligomeric species in the discharge, which can, depending on their energies and masses, either take part to thin film growth or be responsible for ablation and densification of the already deposited material. Similarly, Buddhadasa and Girard-Lauriault [18] conclude on the importance of the hydrocarbon molecule structure in NH_3/C_xH_y mixtures on the resultant polymer cross-link density and thus on the stability of the plasma layer.

In this context, we aim, in this work, to compare the use of a single monomer (cyclopropylamine) with the use of a gas mixture (ammonia/ethylene) in order to better understand how the precursor mixture influences the PPFs chemistry and to conclude on the best choice for obtaining NH_2-rich PPFs. To be consistent, we choose to keep the same nitrogen to carbon ratio in the precursor flow rate. In addition to thin film synthesis and characterization, optical emission spectroscopy and mass spectrometry are employed to support our description of the PPF growth mechanism.

2. Experimental

The plasma polymer films (PPFs) are deposited on intrinsic, two faces polished silicon wafers ((100) orientation, thickness 500–550 μm) from Siltronix, which are infrared-transparent in the 1500–4000 cm^{-1} region. Prior to deposition, substrates are cleaned with methanol and dried with nitrogen. PPFs are synthesized from cyclopropylamine (Alfa Aesar, purity 98%) and ammonia/ethylene (Air Liquide, purity >99.9%) mixture.

The deposition chamber used in this study is a cylindrical stainless steel vacuum chamber, which is described and sketched in references [22–24]. The chamber is pumped to a residual pressure of 8×10^{-4} Pa before to introduce the precursors. CPA is progressively heated from 318 K (container) to 328 K (manifold) until 333 K (line) before to be introduced as a vapor in the deposition chamber, thanks to a Minisource injection system from Omicron. Gas flow rate are fixed at 20 sccm (standard cubic centimeters per minute) for CPA and 20 sccm/30 sccm for the NH_3/C_2H_4 mixture, in order to have the same N/C = 1/3 ratio. The working pressure is regulated at 2.66 Pa. The substrates are located at 10 cm from the copper coil connected to the RF power supply (13.56 MHz) and kept at the floating potential during the depositions. All thin films are synthesized in continuous wave mode.

Deposition rates are measured with a Dektak150 mechanical profilometer from Veeco, using a diamond tip with a 2.5 μm curvature radius and an applied force of 0.1 mN.

Fourier transform infrared spectroscopy (FTIR) analyses are performed in transmission mode with a FTIR Bruker IFS 66 V/S spectrometer. Spectra are only measured in the 1500–4000 cm^{-1} region to avoid perturbations by the strong absorption peaks coming from the Si wafer below 1500 cm^{-1}, which could lead to wrong interpretations. Spectra are acquired using OPUS software with a 4 cm^{-1} resolution and averaged over 32 scans. The spectra are then baseline corrected using a concave rubberband correction with 6 iterations and finally normalized in the 2800–3100 cm^{-1} to more easily compare the relative intensities of the different peaks.

X-ray photoelectron spectroscopy (XPS) analyses are performed using a PHI 5000 VersaProbe (ULVAC-PHI) hemispherical analyzer from Physical Electronics, with a highly focused (beam size 200 μm) monochromatic Al Kα radiation (1486.6 eV, 15 kV, 50 W), at a pressure $< 3 \times 10^{-7}$ Pa. X-ray photoelectron spectra are collected at the takeoff angle of 45° with respect to the electron energy analyzer. Surface charging is compensated by a built-in electron gun (2 eV, 20 μA) and an argon ion neutralizer (10 V). The pass energy is 117.4 eV for survey spectra and 23.5 eV for high resolution spectra. For elemental quantification, each point has been reproduced twice, with <2 at.% deviation between the measured values.

The surface concentration of primary amine groups is determined using the chemical derivatization method with 4-trifluoromethyl benzaldehyde (TFBA, purity 98%, Sigma Aldrich) [17,18,25]. The reaction is carried out in a 2.4 L glass desiccator wherein ~0.5 mL of TFBA are dripped onto a ~1 cm thick layer of glass beads, placed at the bottom of the desiccator. 24 h after deposition, the samples are placed on the porcelain disk of the desiccator. The desiccator is then flushed with an argon flow during 10 min, to remove the air inside, and placed in an oven at 45 °C for 3 h. The primary amine selectivity is calculated using the following equation:

$$\frac{[NH_2]_u}{[N]_u} = \frac{[F]_d}{3 \times [N]_d} \quad (1)$$

where [N] and [F] are the relative concentration of nitrogen and fluorine, respectively, determined by XPS, and the u and d subscripts correspond to “underivatized” and “derivatized” samples, respectively.

Mass spectrometry measurements of the gas phase are performed in residual gas analysis mode (RGA) using a quadrupole HAL EQP 1000 mass spectrometer supplied by Hiden Analytical, and connected to the deposition chamber by a 100 μm extraction orifice located at about 50 cm from the coil. Neutral species entering the mass spectrometer are ionized by electron ionization to allow their detection. The electron energy is fixed at 20 eV in the ionization source of the spectrometer in order to avoid excessive fragmentation of the precursors in the ionization chamber.

Optical emission spectroscopy (OES) measurements are performed using a portable multichannel spectrometer AVS-MC2000–5 from Avantes. 5 different entrance slits allow to study the light from the plasma over 5 different wavelength ranges (200–350 nm, 330–465 nm, 440–610 nm, 590–735 nm and 720–970 nm). Light is collected through an optical fiber located at 10 cm from the coil and connected to the desired slit of the spectrometer depending on the studied wavelength range. Spectra are acquired with an integration time of 300 ms and averaged over 3 measurements.

3. Results and discussion

First, the deposition rates of plasma polymer films (PPFs) synthesized from both cyclopropylamine (CPA) and ammonia/ethylene (AmEt) mixture have been measured as a function of the power injected in the discharge in the range 30–100 W. The measurements are presented in Fig. 1. To compare more easily these data with those found in the literature, the Yasuda parameter W/F [20], corresponding to the energy applied per injected monomer molecule, has been calculated for each condition according to the following equation:

$$\frac{W}{F}(eV) = \frac{W}{\frac{F}{V_m}} \times \frac{1}{N_A} \times \frac{1}{|e|} \quad (2)$$

where W is the power injected in the discharge in W or J s^{-1}, F is the monomer flow rate in L s^{-1}, V_m is the molar volume of the gas (24 L mol^{-1}), N_A is the Avogadro constant (6.02×10^{23} mol^{-1}) and $|e|$ is the modulus of the elementary charge (1.602×10^{-19}), used as a conversion factor between J and eV (Table 1).

For both kinds of precursor, the deposition rates increase with the power in the studied range. This is consistent with a higher energy transfer from the power supply to the species present in the deposition chamber, leading to a stronger fragmentation of the monomers and to a greater number of active radicals and other energetic species that can take part to thin film growth. The fact that the deposition rates

Please cite this article as: C. Vandenabeele, et al., Comparison between single monomer versus gas mixture for the deposition of primary amine-rich plasma polymers, Thin Solid Films (2016), http://dx.doi.org/10.1016/j.tsf.2016.08.008

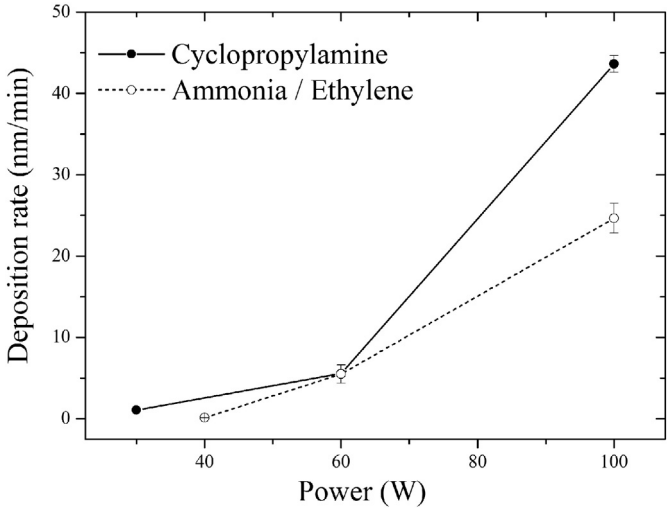

Fig. 1. Deposition rates as a function of the power obtained for both CPA and AmEt discharges.

continuously increase indicates that the monomer-deficient domain [20,26] has not been reached in the studied range of power.

At 30 W, the deposition rate in the case of AmEt is so slow that it has not been possible to measure it, even after 5 h of deposition. Therefore, the deposition rate at 40 W has been measured instead. Except at 60 W, where the deposition rates are similar for both kinds of precursor, the plasma polymer films (PPFs) grow faster with CPA. This phenomenon can be explained by different reasons. First, unreported mass spectrometry (MS) measurements of the gas phase show that unfragmented CPA molecules are still present in the discharge, even at 100 W. Thus, bigger species can take part to thin film growth in this case, which could partly explain the higher deposition rate. Second, the total precursor flow being 2.5 times higher in the case of AmEt (50 sccm) than in the case of CPA (20 sccm), the composite parameter W/F is 2.5 times higher in the case of CPA, because of the longer residence time of CPA molecules in the discharge. Thus, CPA molecules are more activated than ammonia and ethylene molecules, and therefore, more likely to take part to thin film growth.

A third part of the explanation has been deduced from both optical emission spectroscopy (OES) and MS measurements of a pure ammonia discharge (20 sccm, 2.66 Pa, 100 W) performed at two different moments: 1) just after cleaning the chamber inner walls with an Ar/O_2 plasma, monitored by MS, until the signals at $m/z = 18$, 28 and 44 a.u., corresponding respectively to water H_2O, carbon monoxide CO and carbon dioxide CO_2, become weak compare with the signal at m/z = 32 a.u., corresponding to molecular oxygen O_2; 2) after performing a long-time deposition at high power (100 W), until the chamber inner walls are completely coated with PPF. These results are presented in Fig. 2.

When the chamber is clean (Fig. 2a, top), OES measurements performed in the range 330–430 nm only allow to detect the (0, 0) and (1, 1) transitions of the angstrom system ($A^3\Pi$–$X^3\Sigma^-$) of NH at 336.22 and 337.25 nm, respectively, and the bands corresponding to the second positive system ($C^3\Pi_u$–$B^3\Pi_g$) of N_2 such as for example the (0, 0), (1, 2), (0, 1), (1, 3), and (0, 2) transitions at 337.27, 353.81, 357.82, 375.68 and 380.56 nm, respectively [27]. However, when the chamber inner walls are coated with PPF, an additional band clearly appears at 388.36 nm in the OES spectrum (Fig. 2a, bottom), which is characteristic of the (0, 0) transition of the violet system ($B^2\Sigma$–$X^2\Sigma$) of CN.

Similarly, only the signals at $m/z = 2$, 16, 17, 18 and 28 a.u. can be detected on the MS spectrum of the pure ammonia discharge after cleaning of the deposition chamber (Fig. 2b, top), corresponding to H_2^+, NH_2^+, NH_3^+, NH_4^+ and N_2^+ ions. Additional signals appears at $m/z = 26$, 27 and 29 a.u. when the chamber walls are coated with PPF (Fig. 2b, bottom), likely corresponding to CN^+, HCN^+ and H_3CN^+ ions. Besides, we can note that the ratio I_{17}/I_{28} corresponding to the intensity at m/z = 17 divided by the intensity at m/z = 28 decreases from 14.8 to 5.1 between after and before Ar/O_2 cleaning, indicating that another species appears at m/z = 28 when the walls are PPF-coated, and revealing the possible presence of H_2CN^+ ions.

Thus, these results indicate that when the chamber is clean, ammonia molecules only undergo dehydrogenation, which leads to the formation of NH_2 and NH radicals, but also of N isolated atoms that can combine together to form N_2 molecules. When the inner walls of the chamber are coated with PPF, all these radicals can react with the deposited material to form H_xCN species, with x = 0 to at least 3, leading either to the formation of active radicals that can assemble together in the gas phase or be adsorbed on any surface inside the deposition chamber, or to the formation of stable species like N_2 or HCN that can be pumped out the deposition chamber. In this last case, the NH_3 discharge can be considered as an etching plasma responsible for an ablation of the growing PPF.

Therefore, the above-mentioned reasons can explain why PPFs grow faster with CPA than with the AmEt mixture. A last observation that can be done in Fig. 1 is the strong increase in deposition rates between 60 and 100 W. This feature can also be explained by performing OES measurements. Indeed, by integrating the total light emitted by CPA and AmEt discharges in the 200–970 nm range, we can see in Fig. 3 a strong increase in luminosity between 60 and 100 W.

This strong increase in luminous intensity is characteristic of the capacitive-to-inductive (E-to-H) transition that occurs in such reactor configuration, where the plasma is initiated by a radiofrequency current flowing through a coil [28,29]. The E-to-H transition takes place when the electromotive force induced by the variations of the magnetic field generated by the RF current flowing through the coil becomes high enough to transfer a sufficient energy to the electrons for ionizing the gas. This E-to-H transition is therefore characterized by a strong increase in electron density in the plasma, which is accompanied by a strong increase in radiative species density, precursor fragmentation and consequently, growth rate of PPFs. The fact that the deposition rates are similar for both kinds of precursor only at 60 W could be explained by an E-to-H transition arising at a lower power in the case of the AmEt mixture. However, an accurate determination of the power at which the E-to-H transition occurs for each gas mixture being beyond the scope of this paper, this hypothesis has not been validated.

Based on these deposition rate measurements, 100 nm-thick PPFs have been deposited for both kinds of precursor and for each power, except for the AmEt PPF at 40 W, whose thickness has been limited to 30 nm because of the very low deposition rate in this condition. All the films have then been analyzed by XPS (combined with chemical derivatization with TFBA) and FTIR.

The relative surface concentrations of detected elements, determined by XPS for both underivatized and TFBA-derivatized samples are gathered in Table 2. Based on these measurements, the [N]/[C] and $[NH_2]$/[N] ratios have been calculated. The evolution of these two ratios as a function of the power injected in the discharge is depicted in Fig. 4.

We can note that both the nitrogen surface concentration and the [N]/[C] ratio are about 50% higher for CPA-based PPFs than for AmEt-based PPFs in similar power conditions. This is likely related to the fact that C—N bonds are already present in the CPA molecule and thus,

Table 1
Calculations of the *W/F* parameter for the different deposition conditions tested.

Injected power (W)	*W/F* (eV)	
	CPA	AmEt
30	22.4	8.9
60	44.8	17.9
100	74.7	29.9

Please cite this article as: C. Vandenabeele, et al., Comparison between single monomer versus gas mixture for the deposition of primary amine-rich plasma polymers, Thin Solid Films (2016), http://dx.doi.org/10.1016/j.tsf.2016.08.008

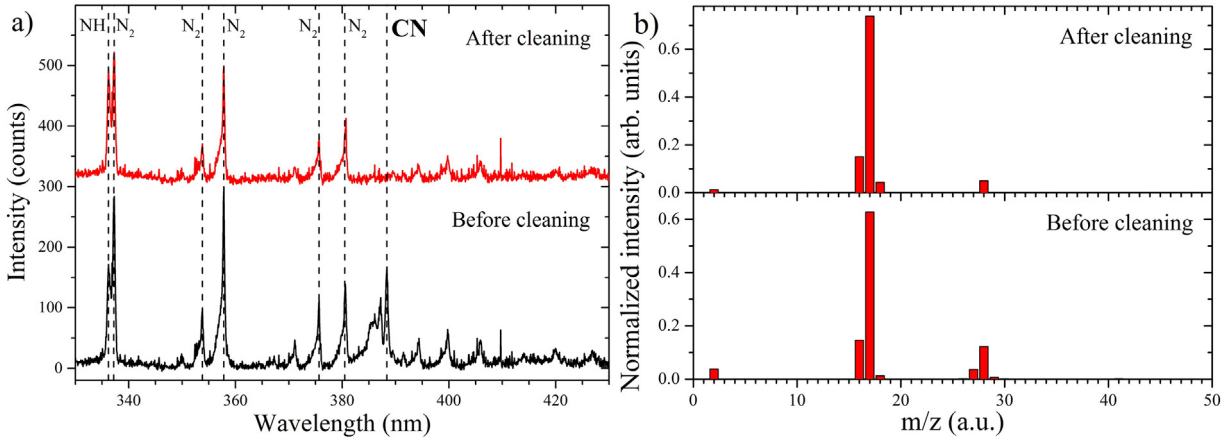

Fig. 2. (a) OES and (b) MS measurements in RGA mode of a pure ammonia discharge (20 sccm, 2.66 Pa, 100 W) performed directly after Ar/O_2 cleaning (top) and after a long PPF deposition (bottom), namely without (top) and with (bottom) PPF deposited on the inner walls of the deposition chamber. For MS results (b), the spectra have been normalized to the total ionic current.

that more species containing C—N bonds are potentially condensable in the CPA-based PPFs.

If the nitrogen content is not affected by the power in the studied range for CPA-based PPFs, it progressively decreases when power increases in the case of AmEt-based PPFs (Fig. 4a). This is attributed to the higher fragmentation that takes place in the AmEt discharge at high power, which increasingly leads to the formation of stable nitrogen-containing molecules, such as N_2 or HCN, which do not take part to the PPF growth. OES analysis reveals, however, that the loss of nitrogen by N_2 formation is more limited in the case of CPA. Indeed, we can see in Fig. 5 that the emission bands at 337.27 and 357.82 nm, corresponding to N_2 molecules, are barely distinguishable in the spectrum of the 100 W CPA discharge. On the contrary, these two bands are much more intense in the AmEt discharge in similar W/F conditions, namely when comparing the 100 W CPA discharge with a 250 W AmEt discharge (Fig. 5b).

Furthermore, we can see in Fig. 4b that the primary amine selectivity $[NH_2]/[N]$ is equivalent for both precursors at powers of 60 and 100 W. However, at lower power, the $[NH_2]/[N]$ ratio becomes much higher using the AmEt mixture. This point is not clearly understood, but a possible explanation could be the fact that the starting molecule containing the primary amine group in the case of AmEt is NH_3, which still contains NH_2 groups after the scission of an N—H bond. Thereby, in mild energetic conditions, the density of NH_2 groups would be higher in the AmEt discharge than in the CPA discharge, resulting in higher primary amine selectivity in AmEt-based PPFs. Nevertheless, density functional theory (DFT) calculations need to be performed to support this hypothesis.

For both gases, the primary amine selectivity decreases with the power. This feature is largely discussed in the literature [6,26] and is attributed to a lower retention of the chemical group of interest when the power increases due to a higher fragmentation of the precursors. The loss of primary amine selectivity can also be observed on FTIR spectra of PPFs illustrated in Fig. 6.

Peaks assignment has been done based on different sources [9, 30–34] that are gathered in Table 3. Amide groups have not been taken into account because XPS depth profiles performed on the different samples show that oxygen is absent from the PPFs bulk. Therefore, the oxygen detected by XPS (Table 2) only comes from post-treatment surface oxidation. As FTIR analysis are performed in transmission mode, the whole film thickness is analyzed and surface functionalities do not have a strong contribution in the absorption bands. This conclusion is supported by the fact that the spectrum related to the AmEt sample at 40 W, being less thick (~30 nm) than the other ones (~100 nm), is much more noisy than the other spectra.

If FTIR is not a suitable technique to quantify NH_2 groups in the samples, because the N—H stretching vibrational modes of primary amine, secondary amine and imine groups are all located in the same region between 3200 and 3500 cm^{-1}, we can note, however, that the intensity of the absorption peaks corresponding to the vibrations of multiple and conjugated CN bonds (1500–1750 and 2100–2300 cm^{-1}) increases with power compared with the intensity of CH vibrations (2800–3100 cm^{-1}). Therefore, for both kinds of precursor, the increase in power promotes the formation of multiple CN bonds. Since for CPA,

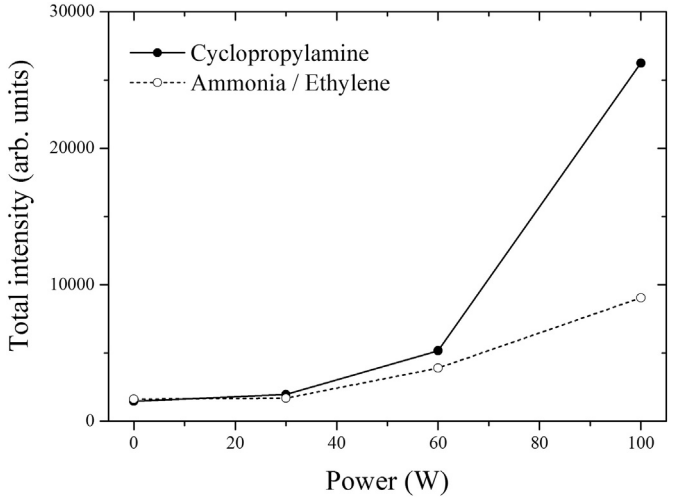

Fig. 3. Evolution of the total intensity of the light emitted by both CPA and AmEt plasmas, as a function of the power. The indicated values correspond to the integration of OES spectra in the range 200–970 nm.

Table 2
Elemental composition measured by XPS at the surface of PPFs synthesized from both CPA and AmEt mixture, before and after chemical derivatization with TFBA, as a function of the power.

Precursor	Power (W)	Elemental composition (at.%)						
		Before derivatization			After TFBA derivatization			
		C1s	N1s	O1s	C1s	N1s	O1s	F1s
AmEt	40	81.7	12.2	6.1	78.2	8.9	6.2	6.7
	60	83.8	11.2	5.0	81.7	10.4	6.0	1.9
	100	83.1	10.6	6.3	82.4	10.3	6.2	1.1
CPA	30	79.7	15.3	5.0	77.7	11.8	5.6	4.9
	60	79.4	15.6	5.0	78.4	13.6	5.3	2.7
	100	79.8	15.1	5.1	79.7	13.9	5.3	1.1

Please cite this article as: C. Vandenabeele, et al., Comparison between single monomer versus gas mixture for the deposition of primary amine-rich plasma polymers, Thin Solid Films (2016), http://dx.doi.org/10.1016/j.tsf.2016.08.008

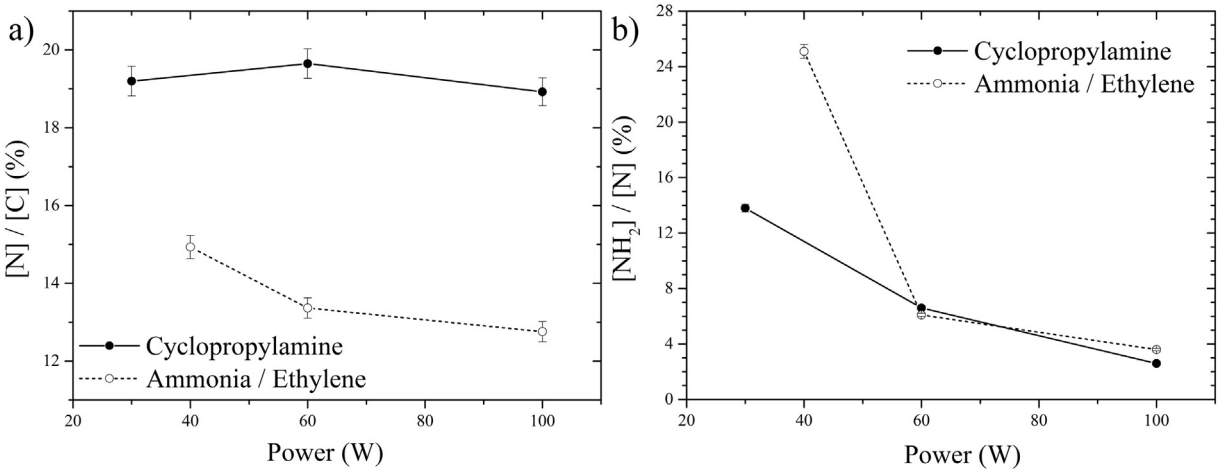

Fig. 4. Evolution of the (a) [N]/[C] and (b) $[NH_2]/[N]$ ratios at the surface of PPFs synthesized from both CPA and AmEt mixture as a function of the power injected in the discharge. [N] and [C] are the elemental composition of nitrogen and carbon, respectively, determined by XPS and indicated in Table 2. $[NH_2]/[N]$ is the primary amine selectivity determined as described in the experimental section.

XPS results show that the nitrogen content is stable in the studied range of power (Fig. 4), an increase in multiple CN bonds content necessarily induces a decrease in primary amine content.

Therefore, the increase with power of the intensity of the peak in the region between 3200 and 3500 cm^{-1} can be attributed to an increase in secondary amine and imine content in the PPFs, confirming the lower retention of NH_2 groups. The vibrational band of NH_2 scissoring mode at 1640 cm^{-1} cannot either be used for primary amine quantification, because this vibration occurs in the same region than the C═N and C═C vibrational modes. Note that if C═C bonds are present in the PPFs, they are mainly in tetrasubstituted configuration, because the associated C—H vibrational bands of alkenes, appearing in the 3000–3100 cm^{-1} region [30, 32], are absent from FTIR spectra. As the NH_2 content decreases with power, the higher relative intensity of the peak around 1640 cm^{-1} likely indicates a higher content of imine groups in the coatings when the power increases. This interpretation is also consistent with the higher relative intensity of the doublet peak between 2100 and 2300 cm^{-1}, corresponding to nitrile C≡N groups, conjugated multiple CN bonds, and possibly cumulated double-bonds compounds such as ketenimine >C═C═N— and carbodi-imine R—N═C═N—R groups. Thereby, the increase in power is responsible for a strong dehydrogenation of the precursor molecules in the gas phase (confirmed by MS results), but probably also a dehydrogenation of the surface of the growing PPF (as stated in reference [12]), which tends to promote the formation of multiple and/or conjugated CN bonds.

It is interesting to note that the evolution of the relative intensities between the different peaks in CPA spectra follow a behavior that is exactly the opposite of that observed by Manakhov et al. [9]. Indeed, they report a higher content of multiple CN bonds, such as nitriles, in low energetic conditions. But as they work in a parallel plate electrode configuration at much higher pressure (120 Pa), adding a constant argon flow to the CPA flow, it is difficult to compare our experiments. Moreover, they study the evolution of the chemistry depending on the composite parameter W/F, acting on the duty cycle (in pulsed wave mode) and on the CPA flow rate to vary the energy supplied per CPA molecule, without considering the energy absorbed by Ar atoms. Besides, they do not report chemical derivatization experiments for NH_2 quantification that would have allowed to directly compare our results. Perhaps, they observe an opposite behavior because they do not work with a constant gas mixture and probably because their high energetic conditions are not those where the highest energy transfer to CPA molecules occurs. Indeed, we can notice that they measure lower deposition rates when the W/F parameter increases, which is not the general trend in a plasma polymerization process, except in the monomer-deficient regime or under high energetic conditions, when ion-induced etching reactions lead to an ablation phenomenon [26].

We can also observe in Fig. 6 that the PPF chemistry strongly differs depending on the kind of precursor used. Indeed, much less multiple and conjugated CN bonds are present in the case of AmEt-based PPFs compared with CPA-based PPFs. This feature cannot be simply

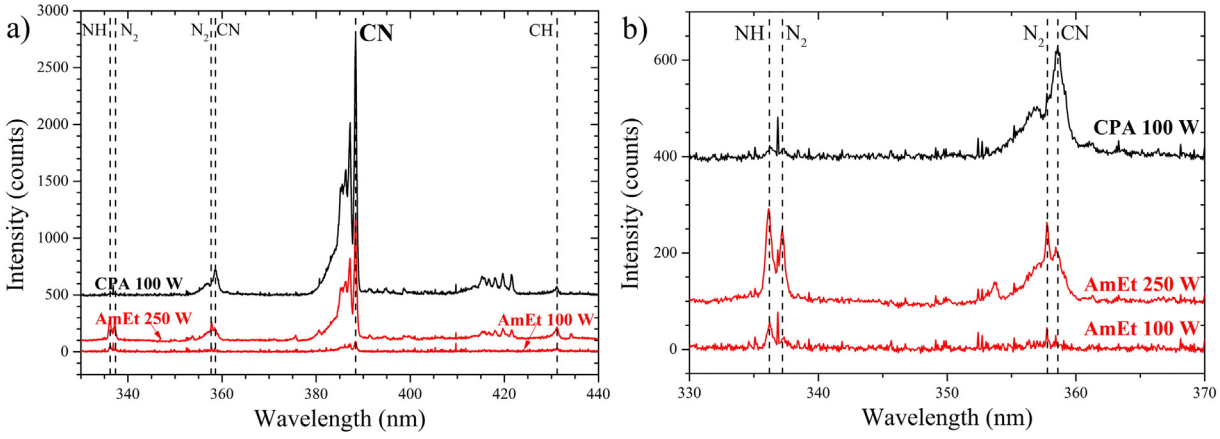

Fig. 5. (a) Comparison between OES spectra of CPA and AmEt discharges at 100 W (the spectra of an AmEt discharge at 250 W is also sketched for a comparison between AmEt and CPA discharges with the same W/F ratio); (b) Zoom in the 330–370 nm range.

Please cite this article as: C. Vandenabeele, et al., Comparison between single monomer versus gas mixture for the deposition of primary amine-rich plasma polymers, Thin Solid Films (2016), http://dx.doi.org/10.1016/j.tsf.2016.08.008

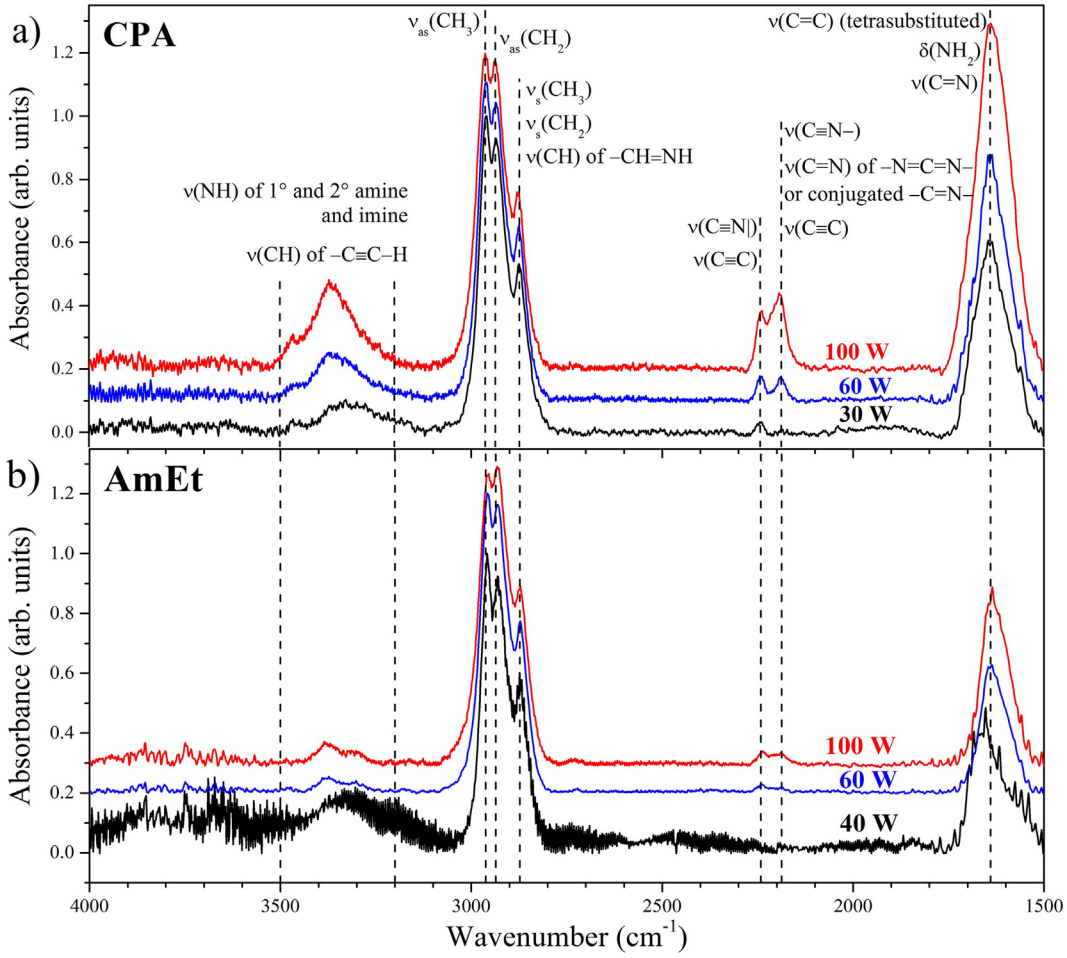

Fig. 6. FTIR spectra recorded in transmission mode of PPFs synthesized from (a) CPA and (b) AmEt mixture at different powers. Spectra are normalized in the region 3100–2800 cm^{-1} to allow an easier comparison of the relative intensities of the different peaks. Spectra are also shifted to separate the curves. Peaks assignment has been done based on different sources that are gathered in Table 3.

explained by the fact that there is a higher nitrogen content in the films synthesized from CPA, because the nitrogen content in CPA-based PPFs is only ~ 50% higher than in AmEt-based PPFs (Table 2), whereas the intensity of the C≡N absorption band at 2242 cm^{-1} is 4.5 times higher in the case of CPA, by comparing the spectra at 100 W (Fig. 6). The higher nitrile content observed with CPA is more likely related to the difference in monomers structure. Indeed, by performing density functional theory (DFT) calculations, Denis et al. [17] have shown that the most energetically favorable reaction that occurs in the CPA discharge is the ring opening, which leads to the formation of extremely reactive biradicals that retain C—N bonds and NH_2 groups, promoting their incorporation in the PPF. On the contrary, they have shown that the C—N bond breaking is the most likely reaction occurring in an AA discharge, due to the high stability of allyl radicals. Based on these calculations, we can think that the ring present in the CPA molecule also promotes the formation of nitrile functionalities by stabilizing C—N bonds, whereas the absence of C—N bonds, as well as the possibility for ammonia molecules to etch the surface of the growing PPFs, strongly decrease the possibility to generate nitrile groups in the case of the AmEt mixture. For the time being, this hypothesis has not been validated by DFT calculations, but it will be checked in the future.

The higher content of nitrile groups in CPA-based PPFs can be directly related to the higher content of cyanide radicals in the CPA discharge. Indeed, although the C/N ratio is the same for both precursor flow rates, a much higher content of C≡N radicals is present in the CPA discharge in similar conditions of injected power, as evidenced by the OES measurements reported in Fig. 5a for 100 W discharges. We can see that for the 100 W CPA discharge, the (0, 0) transition of the violet system of CN at 388.36 nm is, by far, the most intense band in the 330–440 nm region, whereas this band is, comparatively, barely visible in the case of the 100 W AmEt discharge. The higher CN content in the CPA discharge is not either due to the higher W/F ratio. Indeed, we can see that the intensity I_{CN} of the CN emission band at 388.36 nm is 29 times higher than the intensity I_{CH} of the (0, 0) transition of the angstrom system ($A^2\Delta$–$X^2\Pi$) of CH at 431.19 nm [27] in the 100 W CPA discharge, whereas it is only 8 times higher in the 250 W AmEt discharge. Thus, a higher content of CN radicals is well present in the CPA discharge.

To further study the relationship between nitrile groups in the PPFs and cyanide radicals in the discharge, additional OES measurements have been performed. More precisely, the evolution of the intensity of the CN line at 388.36 nm has been measured as a function of the treatment time (therefore, we performed a kind of time-resolved OES analysis) for both CPA and AmEt discharges, after having taken care to previously clean the deposition chamber before the experiments with an Ar/O_2 plasma as previously described. The results show that the CN line intensity increases with time, as depicted in Fig. 7.

In Fig. 7b, we can see that the CN line intensity is multiplied by 3.8 between 10 and 1200 s of treatment time when the chamber is initially clean in the case of a 100 W CPA discharge. The CN line intensity strongly increases in the first 100 s of treatment time and grows more moderately thereafter, until reaching a plateau after 600 s. The fact that CN species are detected directly after plasma ignition indicates that cyanide radicals are formed in the gas phase within the first few seconds of the

Please cite this article as: C. Vandenabeele, et al., Comparison between single monomer versus gas mixture for the deposition of primary amine-rich plasma polymers, Thin Solid Films (2016), http://dx.doi.org/10.1016/j.tsf.2016.08.008

Table 3
Peaks assignment found in the literature for the absorption bands observed in Fig. 6. The values between brackets correspond to the position of vibrational bands in cm^{-1}.

Wavenumber (cm^{-1})	Vibrational modes
3500–3200	NH_2 asym. str. (3430) [9], (3380–3350) [30], (3363) [31] NH_2 sym. and NH str. (3365) [9] NH_2 sym. str. (3310–3280) [30] NH str. of 1° amine (3450–3160) [32] NH str. of 2° amine (3320–3280) [30], (3500–3300) [32] N—H str. of imine (3356) [33], (3400–3300) [32] N—H str. of 1° and 2° amine (3350) [34] C—H str. of alkynes (3350–3250) [30], (3340–3280) [32]
2962	CH_3 asym. str. (2965) [9], (2962 ± 10) [30], (2985) [34], (2948) [31], (2975–2950) [32]
2935	CH_2 asym. str. (2930) [9], (2926 ± 10) [30], (2940) [34], (2928) [31], (2940–2915) [32]
2873	CH_3 and CH_2 sym. str. (2870) [9] CH_3 sym. str. of alkanes (2872 ± 10) [30], (2885) [34], (2885–2865) [32] CH_2 sym. str. of alkanes (2855 ± 10) [30], (2850) [34], (2870–2840) [32] C—H str. of imine (2860) [33], (2870) [31]
2242, 2187	C ≡ N str. (2245) [9,34], (2260–2240) [30], (2190) [33], (2182) [31], (2260–2200) [32] C≡N— and —N═C═N— str. (2190) [9] C≡N— str. (2175–2110) [32] Asym. C═C═N str. of ketenimines >C═C═N— (2170–2000) [32] Asym. N═C═N str. of carbodi-imines (2155–2130) [32] Mono. (2150–2100) and disubstituted (2260–2190) C≡C str. [30,32] Conjugated C≡C with C═C and C≡C (2270–2200) [32] Conjugated —C═N— (2200) and C≡N (2222) [34]
1640	C═N str. (1690–1640) [9], (1630) [33,34], (1635) [31], (1690–1630) [32] —NH_2 scissor. (1640) [9], (1650–1580) [30,32] Tetrasubstituted C═C str. (1680–1665) [30], (1690–1670) [32] C═C str. of >C═C—N< (1680–1630) [32]

treatment. Nevertheless, the strong increase in CN line intensity that occurs over time reveals the appearance of a new source of cyanide groups, implying to take into account another mechanism of C≡N production. The most likely mechanism is the formation of nitrile groups on the surface of the growing PPF by adsorption of nitrogen-containing species on the surface, which undergo dehydrogenation due to different phenomena (electronic and ionic bombardment, UV irradiation, heating of the surface). This leads, after surface rearrangements, to the formation of nitrile groups that are finally etched to enrich the content of cyanide radicals in the discharge. The CN line intensity reaches a plateau once the production and etching rates of nitrile groups on the PPF surface stabilize.

To be sure that the evolution of the CN line intensity is not only due to the rise in temperature that arises over time, the same experiment has been reproduced 2 h later, to let the chamber walls cool down, without cleaning meantime the deposition chamber, therefore with PPF initially present on the inner walls of the reactor. We can see in Fig. 7b that in this case, the CN line intensity directly reaches a plateau after a few seconds of treatment, which supports the formulated hypothesis.

In Fig. 7c, we can see that the same behavior is observed in the case of a 250 W AmEt discharge, except for a few details. Indeed, the CN line intensity increases over time (multiplied by 4.7 between 10 and 1200 s) and it rapidly reaches its maximum value when the chamber is not initially clean. However, we can see that it takes much more time to reach the plateau region in the case of the AmEt discharge, although it is not possible to give the final value reached in the plateau region, because the CN line intensity does not cease to grow with time. These results are consistent with the fact that the formation of nitrile groups on the AmEt-based PPFs surface is more difficult than in the case of CPA. Probably in this case, the rise in temperature occurring over time helps the formation of nitrile groups and much more time is required to stabilize the production and etching rates of C≡N bonds.

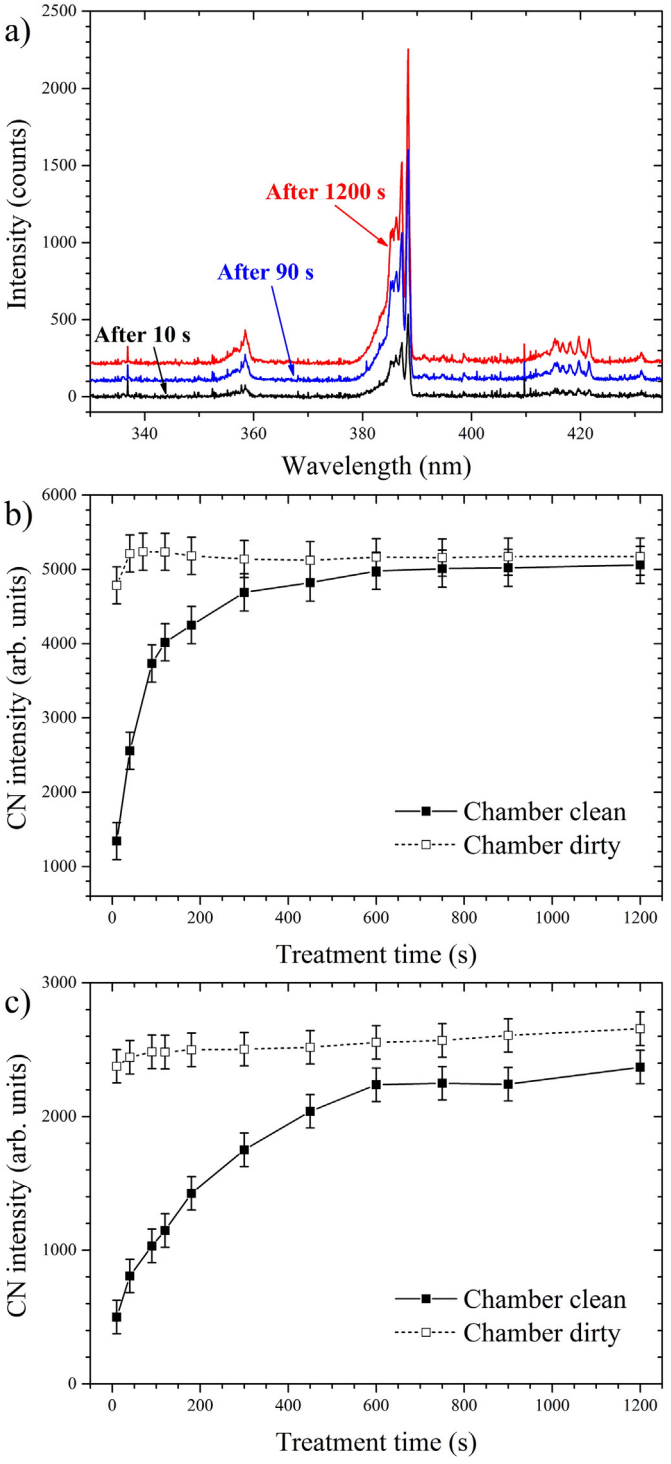

Fig. 7. (a) OES spectra of a 100 W CPA discharge for different treatment times. Ar/O_2 cleaning of the deposition chamber has been performed before to switch on the CPA discharge, to remove the deposited material on the reactor inner walls. (b) Evolution of the CN line intensity of a 100 W CPA discharge and of a (c) 250 W AmEt discharge as a function of the treatment time when the deposition chamber is clean and when the inner walls of the reactor are coated with PPF. The CN line intensity has been determined by integrating the peak area between 376 and 390 nm.

4. Conclusions

In this work, we show that the choice of precursors, either single monomer or gas mixture, strongly influences the plasma polymerization mechanisms and thus, the final properties of the deposited coatings.

Please cite this article as: C. Vandenabeele, et al., Comparison between single monomer versus gas mixture for the deposition of primary amine-rich plasma polymers, Thin Solid Films (2016), http://dx.doi.org/10.1016/j.tsf.2016.08.008

The use of cyclopropylamine (CPA) leads to higher deposition rates and nitrogen incorporation in the film compared with the use of an ammonia/ethylene (AmEt) mixture in similar energetic conditions and for a same C/N ratio in the precursor flow rate. This is attributed to the presence of larger condensable fragments that initially contain C—N bonds in the CPA discharge. The nitrogen incorporation is constant in the studied range of power for CPA, but decreases when the power increases in the case of AmEt. This is probably because of the production of stable molecular nitrogen N_2 from ammonia in the AmEt discharge, which is then pumped out the deposition chamber. The production of N_2 is much more limited in the case of CPA.

Whatever the gas mixture, the $[NH_2]/[N]$ ratio decreases when the power increases because of the increased dehydrogenation of both monomer molecules in the gas phase and surface of the growing PPFs. This dehydrogenation promotes the formation of multiple CN bonds (possibly conjugated) and cumulated CN double bonds, at the expense of primary amine retention. Etching reactions of nitriles groups on PPFs surface are evidenced, leading to the release in the discharge of cyanide radicals.

A higher presence of multiple CN bonds is observed in the CPA-based layers, leading to a higher content of cyanide radicals in the CPA discharge. This is possibly related to the initial structure of the CPA molecule that tends to conserve the C—N bond, while preliminary results of a more complete plasma diagnostic, implying gas phase FTIR and additional MS measurements, seems to indicate that ammonia and ethylene do not react together in the gas phase and are therefore incorporated separately in the PPF. Since NH_3 is responsible for an etching effect of the deposited material, it lowers again the probability to generate C—N bonds, and probably nitrile groups. This more complete plasma diagnostic will be discussed in a future work.

Acknowledgements

The authors would like to convey their deepest gratitude to the Belgian Government (Belspo) through the "Pôle d'Attraction Interuniversitaire" (PAI, P7/34, "Plasma-Surface Interaction", Ψ) for financial support.

References

[1] H.J. Griesser, R.C. Chatelier, T.R. Gengenbach, G. Johnson, J.G. Steele, Growth of human cells on plasma polymers: Putative role of amine and amide groups, J. Biomater. Sci. Polym. Ed. 5 (1994) 531–554.
[2] M. Müller, C. Oehr, Plasma amino functionalisation of PVDF microfiltration membranes: Comparison of the in plasma modifications with a grafting method using ESCA and an amino-selective fluorescent probe, Surf. Coat. Technol. 116–119 (1999) 802–807.
[3] R. Nakamura, H. Muguruma, K. Ikebukuro, S. Sasaki, R. Nagata, I. Karube, H. Pedersen, A plasma-polymerized film for surface plasmon resonance immunosensing, Anal. Chem. 69 (1997) 4649–4652.
[4] A. Manakhov, E. Makhneva, P. Skládal, D. Nečas, J. Čechal, L. Kalina, M. Eliáš, L. Zajíčková, The robust bio-immobilization based on pulsed plasma polymerization of cyclopropylamine and glutaraldehyde coupling chemistry, Appl. Surf. Sci. 360 (2016) 28–36.
[5] E. Makhneva, A. Manakhov, P. Skládal, L. Zajíčková, Development of effective QCM biosensors by cyclopropylamine plasma polymerization and antibody immobilization using cross-linking reactions, Surf. Coat. Technol. 290 (2016) 116–123.
[6] K.S. Siow, L. Britcher, S. Kumar, H.J. Griesser, Plasma methods for the generation of chemically reactive surfaces for biomolecule immobilization and cell colonization - a review, Plasma Process. Polym. 3 (2006) 392–418.
[7] J.-C. Ruiz, A. St-Georges-Robillard, C. Thérésy, S. Lerouge, M.R. Wertheimer, Fabrication and characterisation of amine-rich organic thin films: Focus on stability, Plasma Process. Polym. 7 (2010) 737–753.
[8] A.A. Meyer-Plath, B. Finke, K. Schröder, A. Ohl, Pulsed and cw microwave plasma excitation for surface functionalization in nitrogen-containing gases, Surf. Coat. Technol. 174–175 (2003) 877–881.
[9] A. Manakhov, L. Zajíčková, M. Eliáš, J. Čechal, J. Polčák, J. Hnilica, Š. Bittnerová, D. Nečas, Optimization of cyclopropylamine plasma polymerization toward enhanced layer stability in contact with water, Plasma Process. Polym. 11 (2014) 532–544.
[10] A. Harsch, J. Calderon, R.B. Timmons, G.W. Gross, Pulsed plasma deposition of allylamine on polysiloxane: A stable surface for neuronal cell adhesion, J. Neurosci. Methods 98 (2000) 135–144.
[11] L. Denis, D. Cossement, T. Godfroid, F. Renaux, C. Bittencourt, R. Snyders, M. Hecq, Synthesis of allylamine plasma polymer films: Correlation between plasma diagnostic and film characteristics, Plasma Process. Polym. 6 (2009) 199–208.
[12] J. Ryssy, E. Prioste-Amaral, D.F.N. Assuncao, N. Rogers, G.T.S. Kirby, L.E. Smith, A. Michelmore, Chemical and physical processes in the retention of functional groups in plasma polymers studied by plasma phase mass spectroscopy, Phys. Chem. Chem. Phys. 18 (2016) 4496–4504.
[13] A. Choukourov, H. Biederman, D. Slavinska, M. Trchova, A. Hollander, The influence of pulse parameters on film composition during pulsed plasma polymerization of diaminocyclohexane, Surf. Coat. Technol. 174–175 (2003) 863–866.
[14] C.G. Gölander, M.W. Rutland, D.L. Cho, A. Johansson, H. Ringblom, S. Jönsson, H.K. Yasuda, Structure and surface properties of diaminocyclohexane plasma polymer films, J. Appl. Polym. Sci. 49 (1993) 39–51.
[15] T.R. Gengenbach, R.C. Chatelier, H.J. Griesser, Correlation of the nitrogen 1 s and oxygen 1 s xps binding energies with compositional changes during oxidation of ethylene diamine plasma polymers, Surf. Interface Anal. 24 (1996) 611–619.
[16] K. Vasilev, L. Britcher, A. Casanal, H.J. Griesser, Solvent-induced porosity in ultrathin amine plasma polymer coatings, J. Phys. Chem. B 112 (2008) 10915–10921.
[17] L. Denis, P. Marsal, Y. Olivier, T. Godfroid, R. Lazzaroni, M. Hecq, J. Cornil, R. Snyders, Deposition of functional organic thin films by pulsed plasma polymerization: A joint theoretical and experimental study, Plasma Process. Polym. 7 (2010) 172–181.
[18] M. Buddhadasa, P.-L. Girard-Lauriault, Plasma co-polymerisation of ethylene, 1,3-butadiene and ammonia mixtures: Amine content and water stability, Thin Solid Films 591 (2015) 76–85.
[19] A. Contreras-García, M.R. Wertheimer, Low-pressure plasma polymerization of acetylene–ammonia mixtures for biomedical applications, Plasma Chem. Plasma Process. 33 (2012) 147–163.
[20] H. Yasuda, Plasma Polymerization, Academic Press, Orlando, 1985.
[21] H. Biederman, Plasma Polymer Films, Imperial College Press, London, 2004.
[22] S. Ligot, M. Guillaume, P. Gerbaux, D. Thiry, F. Renaux, J. Cornil, P. Dubois, R. Snyders, Combining mass spectrometry diagnostic and density functional theory calculations for a better understanding of the plasma polymerization of ethyl lactate, J. Phys. Chem. B 118 (2014) 4201–4211.
[23] S. Ligot, M. Guillaume, P. Raynaud, D. Thiry, V. Lemaur, T. Silva, N. Britun, J. Cornil, P. Dubois, R. Snyders, Experimental and theoretical study of the plasma chemistry of ethyl lactate plasma polymerization discharges, Plasma Process. Polym. 12 (2015) 405–415.
[24] S. Ligot, D. Thiry, P.-A. Cormier, P. Raynaud, P. Dubois, R. Snyders, In situ IR spectroscopy as a tool to better understand the growth mechanisms of plasma polymers thin films, Plasma Process. Polym. 12 (2015) 1200–1207.
[25] P.-L. Girard-Lauriault, P.M. Dietrich, T. Gross, T. Wirth, W.E.S. Unger, Chemical characterization of the long-term ageing of nitrogen-rich plasma polymer films under various ambient conditions, Plasma Process. Polym. 10 (2013) 388–395.
[26] D. Thiry, S. Konstantinidis, J. Cornil, R. Snyders, Plasma diagnostics for the low-pressure plasma polymerization process: A critical review, Thin Solid Films 606 (2016) 19–44.
[27] R.W.B. Pearse, A.G. Gaydon, The Identification of Molecular Spectra, fourth ed. Chapman and Hall Ltd, London, 1976.
[28] D. Thiry, N. Britun, S. Konstantinidis, J.-P. Dauchot, M. Guillaume, J. Cornil, R. Snyders, Experimental and theoretical study of the effect of the inductive-to-capacitive transition in propanethiol plasma polymer chemistry, J. Phys. Chem. C 117 (2013) 9843–9851.
[29] P. Chabert, N. Braithwaite, Physics of Radio-Frequency Plasmas, Cambridge University Press, Cambridge, 2011.
[30] B.C. Smith, Infrared Spectral Interpretation: A Systematic Approach, CRC Press, Boca Raton, 1999.
[31] A. Abbas, C. Vivien, B. Bocquet, D. Guillochon, P. Supiot, Preparation and multi-characterization of plasma polymerized allylamine films, Plasma Process. Polym. 6 (2009) 593–604.
[32] G. Socrates, Infrared and Raman Characteristic Group Frequencies: Tables and Charts, John Wiley and Sons, Chichester, 2004.
[33] V. Krishnamurthy, I.L. Kamel, Y. Wei, Analysis of plasma polymerization of allylamine by FTIR, J. Polym. Sci., Part A: Polym. Chem. 27 (1989) 1211–1224.
[34] A.E. Lefohn, N.M. Mackie, E.R. Fisher, Comparison of films deposited from pulsed and continuous wave acetonitrile and acrylonitrile plasmas, Plasmas Polym. 3 (1998) 197–209.

Please cite this article as: C. Vandenabeele, et al., Comparison between single monomer versus gas mixture for the deposition of primary amine-rich plasma polymers, Thin Solid Films (2016), http://dx.doi.org/10.1016/j.tsf.2016.08.008